DOI: 10.1002/ejic.201100301

Bis(2-methylbenzimidazolyl)amine-Derived Copper Complexes and Their Antineoplastic Activity

Laura A. Rodríguez Solano,[a] Itzen Aguiñiga,[b] Manuel López Ortiz,[b] Reynaldo Tiburcio,[b] Axel Luviano,[b] Ignacio Regla,[b] Edelmiro Santiago-Osorio,[b] Víctor M. Ugalde-Saldívar,[c] Rubén A. Toscano,[a] and Ivan Castillo*[a]

Keywords: Copper / N ligands / Cytotoxicity / Sulfur / Voltammetry

Copper(II) complexes (**1**–**4**) of tri- or tetradentate bis(2-methylbenzimidazolyl)amine ligands (**L^1**–**L^4**) have been prepared and characterized by spectroscopic methods in solution, as well as in the solid state by X-ray crystallography. The ligands act as tridentate donors towards the cupric ions through one central amine and two benzimidazole N atoms in the solid state; a water ligand and a bridging perchlorate group define the distorted octahedral environments of **2** and **3**. Complex **4** has square-pyramidal coordination geometry, with an additional thioether donor attached to the central N atom in the axial position. Electrospray mass spectrometry characterized the complexes as monomeric in acetonitrile solution. Cyclic voltammetry studies established that amine N benzyl-containing **3** has the highest half-wave redox potential of all of these complexes at –0.08 V (vs. Fc^+/Fc) for the Cu^{2+}/Cu^+ couple. The complexes display dose-dependent cytotoxicity against one human and four murine cancer cell lines. Complexes **3** and **4** have good antiproliferative activity against the human chronic leukemia cell line K562. Moreover, for **3** the proliferation of all malignant cell lines decreases at concentrations lower than the IC_{50} for healthy bone marrow cells.

Introduction

Metal-based drugs have become increasingly relevant as alternatives to the traditional drugs based on organic compounds and natural products.[1] Among these, cisplatin is regarded as one of the most effective therapeutic agents in chemotherapy,[2] despite its high toxicity and the drug resistance phenomena associated with it.[3] Nonetheless, the importance of cisplatin as an anticancer drug triggered a widespread interest in metal complexes as potential medicinal agents,[4] particularly in search of compounds with less severe side effects.

In this context, copper is an appealing candidate to replace platinum in drugs based on its role in biological systems as an essential element,[5] which could render its complexes less toxic. The molecular mechanisms underlying the antitumor activity of copper complexes reported to date are not fully established. Initial hypotheses considered analogies with Pt to propose DNA binding, intercalation, and cleavage activity; proteasome inhibition has been postulated as a possible apoptotic mechanism.[6] Alternatively, evidence for oxidative damage by production of reactive oxygen species (ROS) has also been reported, and a form of nonapoptotic programmed cell death has also been observed.[7] More recently, caspase inhibition leading to paraptotic cell death has also been proposed as a cytotoxic route.[8] These varied cytotoxic mechanisms could circumvent the problem of drug resistance associated with cisplatin. Moreover, the properties of copper complexes are largely dominated by the nature of the ligands,[9] so that fine-tuning can be in principle achieved by ligand modification.

Initial exploration of the biological activity of copper complexes with thiosemicarbazones revealed their potential as antitumor agents.[10] Recent modifications to the ligands have resulted in higher antitumor activity, as well as lower toxicity towards normal cells.[11] A related factor regarding the structure of the ligands is the stability of their copper complexes, as delivery of copper to the target cells can be hampered by sequestering agents that mediate copper trafficking in biological systems. The chelating nature of thiosemicarbazones allow them to strongly bind the copper ions, and it is reasonable to expect that ligands that give rise to highly stable tridentate chelates behave in a similar fashion.

[a] Instituto de Química,
Universidad Nacional Autónoma de México,
Circuito Exterior, Ciudad Universitaria,
México, D.F. 04360, México
Fax: +52-55-56162217
E-mail: joseivan@unam.mx
[b] Facultad de Estudios Superiores Zaragoza,
Universidad Nacional Autónoma de México,
Batalla del 5 de Mayo y Fuerte de Loreto,
México, D.F. 09230, México
[c] Facultad de Química, División de Estudios de Posgrado,
Universidad Nacional Autónoma de México,
Ciudad Universitaria,
México, D.F. 04360, México

Supporting information for this article is available on the WWW under http://dx.doi.org/10.1002/ejic.201100301.

In light of the wide variety of copper complexes that display antitumor activity both in vitro and in vivo, determination of structure–activity relationships is of prime importance.[7a] However, a clear correlation between the biological properties of the complexes and their physical and chemical properties has not emerged to date. Thus far, reports have focused mainly on properties such as the coordination geometry around the copper ions,[12] the oxidation state,[13] redox potentials,[14] and ligating atoms (N, O, P, S). Among nitrogen bases, benzimidazole derivatives display biological activity of their own,[15] which can be modified or enhanced by copper coordination.[16] As a new contribution to this emerging field, we report a series of copper(II) complexes with chelating, tri- and tetradentate bis(2-methylbenzimidazolyl)amine ligands (Scheme 1), which will provide additional data to the existing list of copper compounds with antitumor activity. Moreover, the introduction of different substituents at the central amine allows for the modulation and potential modification of the properties of the complexes. We report their spectroscopic and structural characterization, as well as their antiproliferative activity against murine and human cancer cell lines.

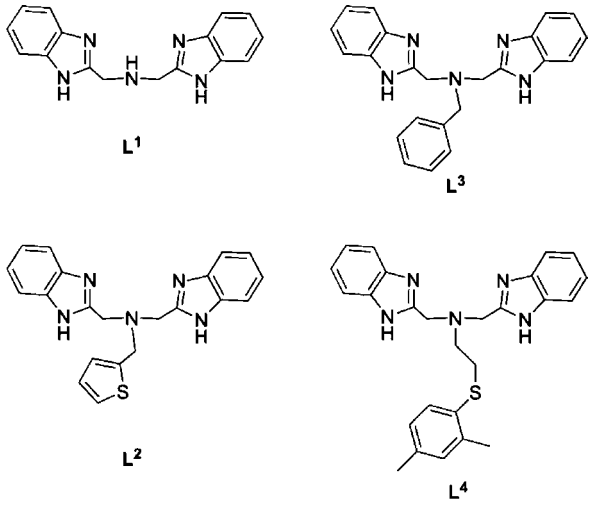

Scheme 1. Bis(benzimidazole)amine ligands $\mathbf{L^1}$–$\mathbf{L^4}$.

Results and Discussion

We recently reported the synthesis of the BOC-protected bis(2-methylbenzimidazolyl)amine ligand precursors $BOC_2\mathbf{L^2}$–$BOC_2\mathbf{L^4}$.[17] Preparation of the complexes entailed the initial deprotection of $BOC_2\mathbf{L^2}$–$BOC_2\mathbf{L^4}$ by treatment with HCl in acetone/water, followed by neutralization with ethanol/water solutions of NaOH or Na_2CO_3. This method allowed the isolation of $\mathbf{L''}\cdot x$HCl ($x \leq 1$) as crystalline solids (Scheme 1). The corresponding copper(II) perchlorate complexes (**1**–**3**) were obtained upon reaction of $Cu(ClO_4)_2\cdot 6H_2O$ with one equivalent of $\mathbf{L''}\cdot x$HCl, or the previously reported $\mathbf{L^1}$.[18] In the case of $\mathbf{L^4}\cdot x$HCl, reaction with $Cu(ClO_4)_2\cdot 6H_2O$ resulted in the formation of a Cu^{II} complex with mixed chloride and perchlorate anions (**4**-Cl), as well as the desired bis(perchlorate) copper complex **4**; analytically pure samples of **4** could not be obtained by this method, and a different synthetic procedure was devised. To this end, the source of chloride was eliminated by adding $Cu(ClO_4)_2\cdot 6H_2O$ as a Lewis acidic deprotecting agent to methanolic solutions of $BOC_2\mathbf{L^4}$. This method afforded **4** in good yields.

Initial characterization of the complexes entailed IR, UV/Vis, and MS analysis. The main features in the IR spectra are the bands between 3550 and 3250 cm^{-1}, which correspond to O–H and N–H stretching modes; the bis(2-methylbenzimidazolyl)amine ligands give rise to C–H stretching bands between 3164 and 2932 cm^{-1}, and the presence of perchlorate anions is evidenced by the strong bands at around 1090–1100 cm^{-1}. The UV/Vis spectra of the complexes in methanolic solutions are characterized by a single d–d transition band (ε in the range of 90–128 $M^{-1}cm^{-1}$) at λ = 695 for **2**, 709 for **3**, and 696 nm for **4**, consistent with square-pyramidal coordination geometry.[19] In the case of **4**, an additional band at λ = 451 nm (ε = 416 M^{-1}) was assigned to the S→Cu ligand-to-metal charge-transfer band based on reports of a related bis(2-methylpyridyl)aminothioether–Cu^{2+} system.[20] An analogous feature is absent in **2**, indicating that the thiophene sulfur atom does not coordinate to the metal center in solution. ESI or FAB^+ mass spectra of all complexes were acquired in acetonitrile/methanol in order to determine their behavior in solution. In all cases the main species detected correspond to monomeric complexes with a 1:1 ligand to metal ratio, without solvent molecules coordinated to the copper ion. In the case of **2**, the FAB^+ mass spectrum is characterized by a peak at m/z = 436, which was assigned to the monocationic species $[(\mathbf{L^2}\text{-H})Cu]^+$. The ESI spectrum for **3** contains peaks at m/z = 429 and 529, assigned to the species $[(\mathbf{L^3}\text{-H})Cu]^+$ and $[\mathbf{L^3}CuClO_4]^+$, respectively. Likewise, analysis of solutions of **4** by FAB^+ MS revealed the presence of the species $[(\mathbf{L^4}\text{-H})Cu]^+$ at m/z = 504. Additionally, all complexes were characterized by EPR spectroscopy in acetone or acetonitrile solutions at 77 K. The observed spectra correspond to axial symmetry, in agreement with UV/Vis spectroscopy, and the complexes are characterized by virtually identical values of $g_\parallel$ = 2.286, $g_\perp$ = 2.069, and $A_\parallel$ = 140.9 G.

The coordination environment around the Cu^{II} centers was established unambiguously by X-ray diffraction analysis. The structure of the related complex $[(\mathbf{L^1})CuCl_2]$ has been reported previously,[21] therefore we decided not to pursue the crystallization of the analogous complex $[(\mathbf{L^1})Cu(ClO_4)_2]$ (**1**). All of the complexes [including $\{(\mathbf{L^1})CuCl_2\}$] feature the bis(benzimidazolyl)amines acting as tridentate ligands; $[(\mathbf{L^1})CuCl_2]$ has a square-pyramidal coordination geometry, with the basal positions occupied by three N atoms and one chloride ligand, and the axial position by the second chloride. In the case of $[(\mathbf{L^2})CuClO_4(H_2O)]ClO_4$ (**2**) and $[(\mathbf{L^3})CuClO_4(H_2O)]ClO_4$ (**3**), the fourth basal position is occupied by a water molecule, with Cu1–O1 bond lengths of 1.983(3) and 1.985(2) Å, respectively. Although both complexes appear to have a distorted square-planar geometry, analysis of the extended structure shows the presence of Cu–O interactions with coordinated perchlorate

anions (Figures 1 and 2), which generate linear coordination polymers characterized by Cu1–O2 and Cu1–O3 distances of 2.443(4) and 2.619(4) for **2** and 2.465(2) and 2.628(2) Å for **3**. Thus, these complexes have distorted octahedral coordination environments, with meridional bis(2-methylbenzimidazolyl)amine ligands, and elongated Cu–O(perchlorate) bonds due to Jahn–Teller effects (see Table 1). Notably, the thiophene sulfur atom of **2** does not coordinate to the Cu^{2+} center [Cu1···S22 distance 5.568(4) Å].

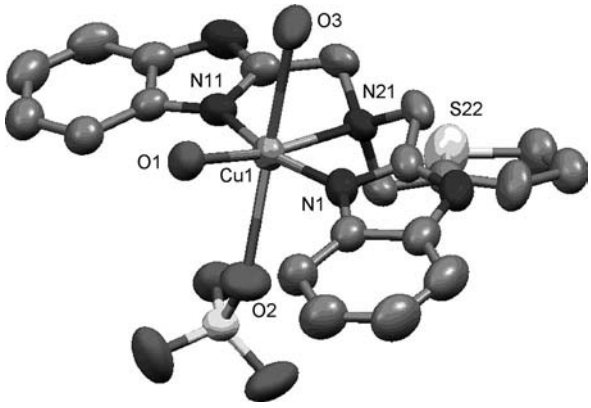

Figure 1. ORTEP diagram of **2** at 50% probability level. Hydrogen atoms, a molecule of water, one perchlorate, and minor-occupancy disordered atoms are omitted for clarity.

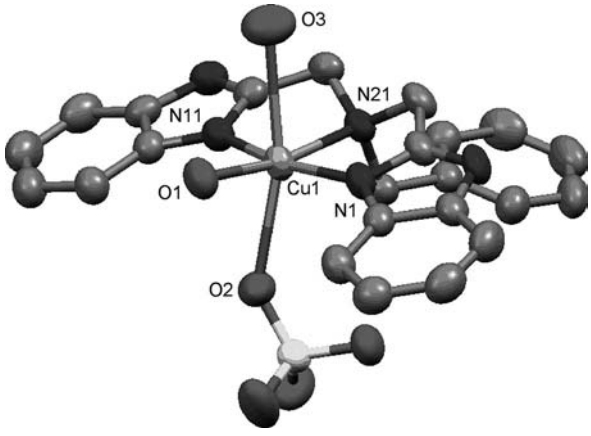

Figure 2. ORTEP diagram of **3** at 50% probability level. Hydrogen atoms, a molecule of water, one perchlorate, and minor-occupancy disordered atoms are omitted for clarity.

Although we were not able to obtain X-ray quality crystals of the bis(perchlorate) Cu^{II} complex of $\mathbf{L^4}$, substitution of one perchlorate for chloride allowed us to establish the solid-state structure of [Cu$\mathbf{L^4}$Cl]ClO_4 (**4**-Cl), which is analogous to bis(2-methylpyridyl)aminothioether–Cu^{2+}.[20] The nitrogen atoms coordinate in a meridional arrangement, as observed for **2** and **3** (Table 1). In contrast to the structure of **2**, complex **4**-Cl has a Cu1–S24 bond [2.749(1) Å] with the thioether arm in an apical position; this Cu–S distance is considerably longer than that reported for bis(2-methylpyridyl)aminothioether–Cu^{2+} [2.604(1) Å].[20] The thioether ligand and the chloride ion in the fourth basal position [Cu1–Cl1 2.277(1) Å], define the square pyramidal geometry around the cupric ion. The additional perchlorate anion does not have significant interactions with the cationic [Cu$\mathbf{L^4}$Cl]$^+$ unit (Figure 3).

Table 1. Selected bond lengths (Å) and angles (°) for complexes **2**, **3**, and **4**-Cl.

Complex **2**			
Cu1–N1	1.943(4)	Cu1–O1	1.983(3)
Cu1–N11	1.943(4)	Cu1–O2	2.443(4)
Cu1–N21	2.112(3)	Cu1–O3	2.619(4)
N1–Cu1–N11	164.26(14)	N11–Cu1–O1	98.76(14)
N1–Cu1–N21	81.96(14)	N11–Cu1–O2	100.92(12)
N11–Cu1–N21	82.35(14)	N11–Cu1–O3	92.67(13)
N1–Cu1–O1	96.38(14)	N21–Cu1–O1	168.40(13)
N1–Cu1–O2	84.81(13)	N21–Cu1–O2	106.93(12)
N1–Cu1–O3	84.23(13)	N21–Cu1–O3	82.90(12)
Complex **3**			
Cu1–N1	1.945(3)	Cu1–O1	1.985(2)
Cu1–N11	1.942(4)	Cu1–O2	2.465(2)
Cu1–N21	2.104(2)	Cu1–O3	2.628(2)
N1–Cu1–N11	164.34(10)	N11–Cu1–O1	96.71(10)
N1–Cu1–N21	82.63(10)	N11–Cu1–O2	87.74(10)
N11–Cu1–N21	81.72(10)	N11–Cu1–O3	82.38(10)
N1–Cu1–O1	98.57(10)	N21–Cu1–O1	169.52(10)
N1–Cu1–O2	97.04(10)	N21–Cu1–O2	105.47(9)
N1–Cu1–O3	95.13(11)	N21–Cu1–O3	83.10(9)
Complex **4**-Cl			
Cu1–N1	1.950(3)	Cu1–Cl1	2.277(1)
Cu1–N11	1.948(3)	Cu1–S24	2.749(1)
Cu1–N21	2.133(4)		
N1–Cu1–N11	161.83(15)	N11–Cu1–Cl1	97.19(10)
N1–Cu1–N21	82.54(14)	N11–Cu1–S24	95.35(10)
N11–Cu1–N21	81.03(14)	N21–Cu1–Cl1	172.68(10)
N1–Cu1–Cl1	98.13(11)	N21–Cu1–S24	83.07(10)
N1–Cu1–S24	90.30(11)	Cl1–Cu1–S24	104.19(4)

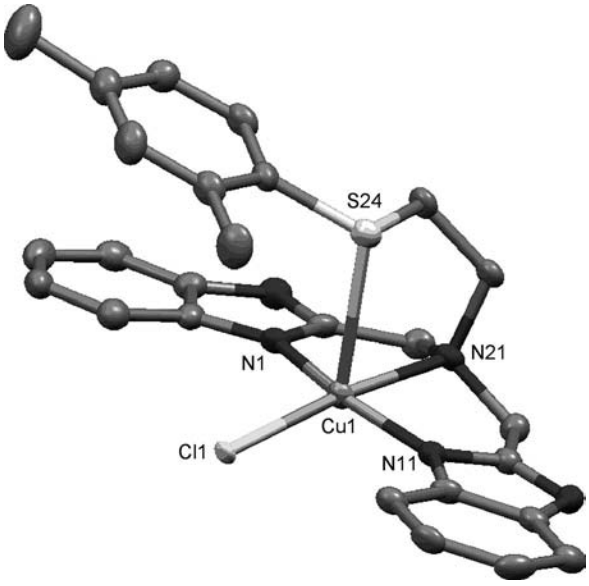

Figure 3. ORTEP diagram of **4**-Cl at 50% probability level. Hydrogen atoms, one perchlorate, and a molecule of water are omitted for clarity.

Antiproliferative Studies

The antiproliferative effect of the complexes was evaluated on murine (WEHI-3, P388, Raw 264.7) and human (K562) leukemia cell lines, as well as on the murine lung fibrosarcoma L929 and healthy murine bone marrow cells. Incubation of the different cell lines with increasing concentrations of the copper complexes revealed a dose-dependent inhibition of cell growth in all cases (Supporting Information, Figures S1 and S2). As a general observation, **1** displays a low inhibitory effect against all cell lines tested, which appears to indicate that the third substituent on the central nitrogen atom is necessary for any significant cytotoxic activity of the complexes. In addition, it can be speculated that the nearly planar arrangement of the two benzimidazole units and the cupric ion is not a requirement for biological activity to be observed, as is the case when DNA intercalation occurs in related bisbenzimidazole[22] or (N-heterocyclic)–Cu systems.[23]

The murine macrophage leukemia cell lines P388 and Raw 264.7 are more sensitive to the thioether-containing complex **4**, whereas myelomonocytic WEHI-3, the human chronic leukemia cell line K562, and the lung sarcoma cell line L929, have comparable sensitivity to all copper complexes at concentrations up to 15 μM. Interestingly, **3**, and to a lesser degree **4**, have a reasonable inhibitory effect on the human cell line K562 compared to the low toxicity exhibited against healthy bone marrow cells (Figure 4 and Table 2). Regarding the cytotoxicity against bone marrow cells, thiophene-derived complex **2** has the highest toxicity, whereas thioether-containing complex **4** has IC_{50} values for all cell lines that are lower or comparable to the value for bone marrow cells, except for K562. Finally, for **3** the proliferation of all cell lines decreases at concentrations lower than the IC_{50} for bone marrow, making it markedly less toxic towards healthy cells. These observations mark **3** as a viable candidate for further modification in order to increase its antiproliferative activity against malignant cell lines, affecting the bone marrow cells only at higher doses. Although the mechanisms of copper entry into the cell are unknown, analogy with cisplatin requires the involvement of the copper transporter 1 protein.[24] An alternative mechanism involves passive diffusion through the hydrophobic cell membrane, which could explain the need of the substituent at the central nitrogen atom resulting in more hydrophobic copper complexes.[8]

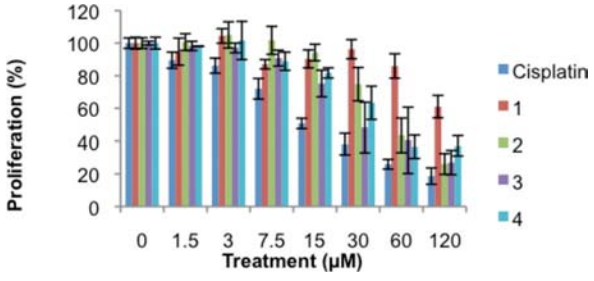

Figure 4. Proliferation inhibition of the human leukemia cell line K562 after treatment with cisplatin and copper complexes **1**–**4**.

Electrochemical Studies

Characterization of the ligands by cyclic voltammetry at a concentration of 1 mM in acetonitrile solution, and a scan rate of 0.200 $V s^{-1}$ revealed several oxidation processes for all of $\mathbf{L^1}$–$\mathbf{L^4}$, and the peaks are distinct from those of the metal-centered redox process (Supporting Information, Figures S3 and S4). The redox potentials for the Cu^{2+}/Cu^{+} couple of the complexes were determined under the same conditions except for **1**, which, due to its poor solubility, was examined at a concentration of 0.6 mM (compared to 1 mM for all other complexes, Table 3). The reduction signals behave reversibly, allowing the determination of the anodic, cathodic, and half-wave potentials ($E_{1/2}$ relative to the Fc^{+}/Fc couple, see Figure 5). The half-wave potential of **1** at $E_{1/2}$ = –0.24 V indicates that it is the most resistant towards reduction from the cupric to the cuprous complex. Complexes **2** and **3** have $E_{1/2}$ values of –0.09 and –0.08 V, respectively, indicating that they can be reduced to the cuprous complexes more easily than **1** or **4**. The half-wave potential of **4** has an intermediate value of –0.12 V. Analysis of the combined data suggests that higher redox potentials, particularly that of **3**, may result in higher cytotoxicity.

Table 3. Redox potentials of complexes **1**–**4** (V, E vs. Fc^{+}/Fc).

Complex	E_{ap}	E_{cp}	$E_{1/2}$
1	–0.16	–0.32	–0.24
2	–0.01	–0.16	–0.09
3	0.04	–0.19	–0.08
4	–0.06	–0.17	–0.12

Thus, these trends indicate that there might be a correlation between the biological activity and the redox potential of the complexes. Copper has been implicated in the generation of ROS, which can be responsible for oxidative damage, leading to cell death.[25] Although further studies are required to test whether that mechanism is operating with the complexes reported here, the ligands employed provide a versatile platform to introduce modifications,

Table 2. IC_{50} values for the different cell lines based on the values presented in Figure 4.

	IC_{50} (μM)					
	P388	K562	WEHI-3	Raw 264.7	L929	Bone marrow
Cisplatin	1.0 ± 0.3	14.9 ± 9.1	2.1 ± 0.6	1.2 ± 0.2	2.4 ± 0.7	2.6 ± 1.7
1	>120 ± 26.0	>120 ± 37.7	54.6 ± 25.9	91.1 ± 22.4	48.7 ± 0.4	>120 ± 2.8
2	66.5 ± 11.9	54.9 ± 9.5	38.0 ± 9.0	34.9 ± 11.3	26.2 ± 11.1	24.6 ± 3.9
3	45.4 ± 12.4	29.33 ± 6.5	22.1 ± 5.2	20.0 ± 2.8	34.5 ± 7.8	48.3 ± 3.5
4	24.4 ± 12.2	45.6 ± 0.9	21.3 ± 3.1	11.1 ± 21.9	24.8 ± 7.0	26.7 ± 10.7

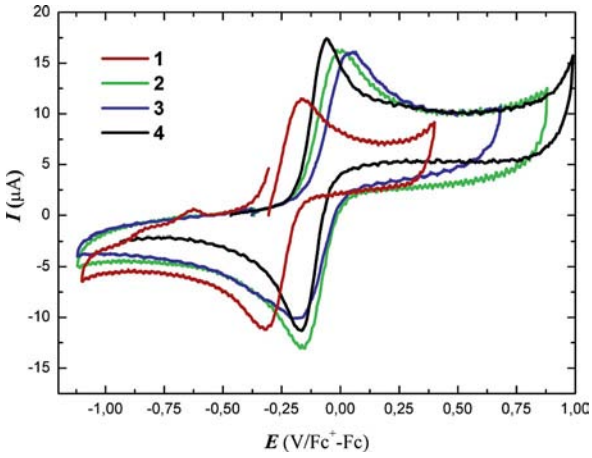

Figure 5. Cyclic voltammograms of in situ prepared cuprous complexes of $\mathbf{L^1}$–$\mathbf{L^4}$, in the potential range relevant to the Cu^{2+}/Cu^{+} redox process.

which could result in complexes that, as in the case of **3**, could be reduced with relative ease, thereby establishing a potential role for cuprous species in antiproliferative activity.

Conclusions

We have synthesized and characterized copper complexes with tri- and tetradentate ligands that share a bis(benzimidazolyl)amine structural motif. These monomeric complexes display dose-dependent cytotoxicity towards one human and several murine cancer cell lines. Based on the antiproliferative activity of the complexes, it is noteworthy that complexes **3** and **4** have an efficiency that, although lower than that of cisplatin against the human leukemia cell line K562, is promising due to the relatively high IC_{50} against healthy bone marrow cells. Both complexes share a common six-membered aromatic ring attached to the central amine, though they differ in the length of the arm connecting the aromatic group to the nitrogen atom, as well as the presence of a thioether linkage in **4**. Modifications at the central nitrogen position could allow us to determine the role of the aromatic group, as well as the potential involvement of sulfur in the biological activity of these complexes. Although it is tempting to propose that the substituent at the central nitrogen atom increases the lipophilicity of the ligand, leading to higher cytotoxicity as recently proposed,[8] further studies are required to verify this hypothesis. With regard to **3**, its low toxicity towards healthy bone marrow cells, mark it as a candidate for structural modifications, which will focus on the introduction of functional groups that could lead to higher redox potentials for the Cu^{2+}/Cu^{+} couple. Ideally, such modifications would result in higher antiproliferative activities against malignant cell lines, while keeping a relatively high IC_{50} for bone marrow cells. The design and development of new benzimidazole-amine derived copper complexes is underway.

Experimental Section

General: The BOC-protected ligands ($BOC_2\mathbf{L}^n$) were prepared according to a literature procedure.[17] All other reagents and solvents were obtained from commercial suppliers, and were used without further purification. Elemental analyses were determined with an Exeter Analytical CE-440 apparatus. UV/Vis spectra were recorded with a Shimadzu UV-160U spectrophotometer; melting points were determined with an Electrothermal Mel-Temp apparatus and are uncorrected; IR spectra were recorded with a Bruker Tensor 27 spectrophotometer in the 4000–400 cm^{-1} region as KBr disks; mass spectra were obtained with a JEOL JMS-SX-102A mass spectrometer at an accelerating voltage of 10 kV, with a nitrobenzyl alcohol matrix and Xenon atoms at 6 keV (FAB^+), or a Bruker Daltonics Esquire 6000 spectrometer with ion trap (Electrospray).

Electrochemical Studies: Measurements were made under a N_2 atmosphere in anhydrous acetonitrile with a potentiostat-galvanostat EG&G PAR model 263A with a glassy carbon working electrode and a platinum wire auxiliary electrode, with $(C_4H_9)_4NPF_6$ as the supporting electrolyte. Potentials were recorded vs. a pseudoreference electrode of AgCl(s)/Ag(wire) immersed in a 0.1 M $(C_4H_9)_4$-NCl acetonitrile solution. The working electrode was polished with alumina, and washed with acetonitrile prior to measurements. All voltammograms were started from the current null potential ($E_{i=0}$) and were scanned in both directions, positive and negative, at a scan rate of 0.200 $V\,s^{-1}$. In agreement with IUPAC convention, the voltammogram of the Fc^+/Fc system was obtained to establish the values of the anodic (E_{ap}) and cathodic (E_{cp}) peak potentials. The electrolytic domain under the working conditions was –2.2 to 3.2 V relative to AgCl(s)/Ag(wire).

EPR Spectroscopy: EPR measurements were made at room temperature or 77 K in quartz tubes with a Jeol JES-TE300 spectrometer operating at X band frequency (9.4 GHz) at 100 KHz field modulation, with a cylindrical cavity (TE_{011} mode). Spectra were acquired in the solid state and in frozen acetone solutions except for **4**, which was acquired in acetonitrile. The external measurement of the static magnetic field was made with a precision gaussmeter Jeol ES-FC5. Spectral acquisition, manipulations, and simulations were performed using the program ESPRIT-382, v1.916.

X-ray Crystallography: Selected crystallographic data are presented in Table 4. Single crystals were mounted at 298 K in a Bruker SMART diffractometer equipped with an Apex CCD area detector. Frames were collected by omega scans, and integrated with the Bruker SAINT software package using the appropriate unit cell.[26] The structures were solved using the SHELXS-97 program[27] and refined by full-matrix least-squares on F^2 with SHELXL-97.[28] Weighted R factors, R_w, and all goodness of fit indicators, S, were based on F^2. The observed criterion of ($F^2 > 2\sigma F^2$) was used only for calculating the R-factors. All non-hydrogen atoms were refined with anisotropic thermal parameters in the final cycles of refinement. Hydrogen atoms were placed in idealized positions, with C–H distances of 0.93 Å and 0.98 Å for aromatic and saturated carbon atoms, respectively. The isotropic thermal parameters of the hydrogen atoms were assigned the values of U_{iso} = 1.2 times the thermal parameters of the parent non-hydrogen atom.

CCDC-796149 (for **2**), -796150 (for **3**), and -796151 (for **4**-Cl) contain the crystallographic data for this article. These data can be obtained free of charge from the Cambridge Crystallographic Data Centre via www.ccdc.cam.ac.uk/data_request/cif.

Ligand Deprotection: To $BOC_2\mathbf{L}^n$ (1 mmol) dissolved in acetone was added HCl (3 M, 4 mL), and the mixture was stirred for 12 h at room temperature. After slow evaporation of acetone, the product

Table 4. Crystal data and structure refinement for compounds **2**, **3**, and **4**-Cl.

	2	**3**	**4**-Cl
Formula	$C_{21}H_{23}Cl_2CuN_5O_{10}S$	$C_{23}H_{25}Cl_2CuN_5O_{10}$	$C_{28}H_{35}Cl_2CuN_5O_6S$
Molecular weight	671.94	665.92	704.11
Crystal system	monoclinic	monoclinic	triclinic
Space group	$P2_1/c$	$P2_1/n$	$P\bar{1}$
Wavelength (Å)	0.71073	0.71073	0.71073
Crystal color	blue	blue	green
T (K)	298(2)	298(2)	100(2)
Crystal dimensions (mm)	0.26× 0.13× 0.12	0.29× 0.26× 0.22	0.20× 0.10× 0.08
a (Å)	10.5263(12)	10.7090(8)	10.903(2)
b (Å)	20.659(2)	20.8148(15)	12.689(3)
c (Å)	13.3535(15)	13.3615(10)	13.101(3)
α (°)	90	90	118.776(3)
β (°)	112.113(2)	112.9150(10)	95.781(3)
γ (°)	90	90	103.916(3)
V (Å^3)	2690.3(5)	2743.3(4)	1491.3(5)
Ranges	$-12 \le h \le 12$	$-12 \le h \le 12$	$-13 \le h \le 13$
	$-24 \le k \le 24$	$-25 \le k \le 25$	$-15 \le k \le 15$
	$-16 \le l \le 16$	$-16 \le l \le 16$	$-15 \le l \le 15$
$\rho_{calcd.}$ (g cm^{-3})	1.659	1.612	1.599
Z	4	4	2
F(000)	1372	1364	744
μ (mm^{-1})	1.152	1.056	1.036
θ range (°)	1.92 to 25.41	1.92 to 25.36	1.83 to 25.36
Absorption correction	empirical	empirical	empirical
T_{max}, T_{min}	0.8983, 0.7709	0.8044, 0.7654	0.9247, 0.8306
Refinement method	full-matrix least-squares on F^2	full-matrix least-squares on F^2	full-matrix least-squares on F^2
Independent reflections	4941	5008	5440
Data/restraints/parameters	4941/276/462	5008/88/425	5440/1/368
Goodness-of-fit on F^2	1.029	1.020	1.038
R	0.0506	0.0429	0.0582
R_w	0.1091	0.0999	0.1431
Largest diff. peak, hole (e Å^3)	0.531, –0.267	0.433, –0.244	0.941, –0.616

crystallized. The solid was collected by filtration and dissolved in water. Na_2CO_3 was added until a pH of 11 was reached, and the precipitate (**L^n**·xHCl, $x < 1$) was collected by filtration and dried under high vacuum.

Synthesis of Complexes: Equimolar amounts of $Cu(ClO_4)_2 \cdot 6H_2O$ and **L^n**·xHCl were dissolved in methanol and stirred for 12 h at room temperature. The solutions were then evaporated under reduced pressure, and the oils were triturated with diethyl ether, filtered, and the solids obtained dried under vacuum.

[CuL^{1}ClO$_4$(MeOH)]ClO$_4$·MeOH (1): **L^1**·xHCl (52 mg, 0.19 mmol), $Cu(ClO_4)_2 \cdot 6H_2O$ (70 mg, 0.19 mmol), methanol (5 mL), light blue solid (88 mg, 0.15 mmol, 76.70%). M.p. 236–238 °C (dec.). $C_{18}H_{23}Cl_2CuN_5O_{10}$ (603.86): calcd. C 35.80, H 3.84, N 11.60; found C 36.04, H 3.83, N 11.28. IR (KBr): $\tilde{\nu}$ = 3274 (strong), 2977, 2931 (weak), 1678, 1629, 1545, 1456, 1412, 1391, 1267 (weak), 1110 (very strong), 928, 851, 756, 694, 625 (weak) cm^{-1}. UV/Vis (d–d transition in MeOH, r.t.): λ_{max} (ε, M^{-1} cm^{-1}) = 752 (78) nm.

[CuL^{2}ClO$_4$(H$_2$O)]ClO$_4$·H$_2$O (2): **L^2**·xHCl (0.10 g, 0.24 mmol), $Cu(ClO_4)_2 \cdot 6H_2O$ (0.10 g, 0.27 mmol), methanol (5 mL), blue solid (0.12 g, 0.17 mmol, 70.83%). M.p. 182–185 °C (dec.). MS (FAB$^+$): m/z = 436 [(**L^2**-H)Cu]$^+$. $C_{21}H_{23}Cl_2CuN_5O_{10}S$ (671.95): calcd. C 37.54, H 3.45, N 9.46; found C 37.69, H 3.50, N 9.84. IR (KBr): $\tilde{\nu}$ = 3530 (strong), 3282 (strong), 3165–3072 (weak), 1623, 1598, 1541, 1478, 1451, 1384, 1332, 1287 (weak), 1091 (very strong), 923, 852, 814, 750, 719, 625, 468 (weak) cm^{-1}. UV/Vis (d–d transition in MeOH, r.t.): λ_{max} (ε, M^{-1} cm^{-1}) = 695 (121) nm. Blue X-ray quality crystals were obtained from crystallization from methanol/water at 4 °C.

[CuL^{3}ClO$_4$(H$_2$O)]ClO$_4$·H$_2$O (3): **L^3**·xHCl (0.20 g, 0.50 mmol), $Cu(ClO_4)_2 \cdot 6H_2O$ (0.20 g, 0.55 mmol), methanol (10 mL) green solid (0.15 g, 0.35 mmol, 70.00%). M.p. 272–278 °C (dec.). MS (ESI): m/z = 429.3 [(**L^3**-H)Cu]$^+$, 529.3 [**L^3**CuClO$_4$]$^+$. $C_{23}H_{25}Cl_2CuN_5O_{10}$ (665.93): calcd. C 41.48, H 3.78, N 10.52; found C 41.19, H 3.72, N 10.15. IR (KBr): $\tilde{\nu}$ = 3541 (strong), 3272 (strong), 3164, 3069, 2953 (weak), 2000–1600, 1598, 1540, 1479, 1453, 1384, 1323, 1287, 1211 (weak), 1090 (very strong), 920, 842, 752, 703, 622, 454, 429 (weak) cm^{-1}. UV/Vis (d–d transition in MeOH, r.t.): λ_{max} (ε, M^{-1} cm^{-1}) = 709 (128) nm. Blue X-ray quality crystals were obtained from crystallization from methanol/water at 4 °C.

[CuL^{4}ClO$_4$(H$_2$O)]ClO$_4$·H$_2$O (4): BOC_2**L^4** (0.38 g, 0.56 mmol), $Cu(ClO_4)_2 \cdot 6H_2O$ (0.21 g, 0.56 mmol), methanol (15 mL), green solid (0.33 g, 0.47 mmol, 83.68%). M.p. 178–183 °C (dec.). MS (FAB$^+$): m/z = 504, [(**L^4**-H)Cu]$^+$. $C_{27}H_{31}Cl_2CuN_5O_9S$ (736.08): calcd. C 44.06, H 4.24, N 9.51; found C 44.06, H 4.41, N 9.42. IR (KBr): $\tilde{\nu}$ = 3328 (strong), 3072, 2978, 2926 (weak), 1763, 1624, 1543, 1478, 1452, 1381, 1323, 1278 (weak), 1101 (very strong), 923, 811, 750, 624, 435 cm^{-1}. UV/Vis (d–d transition in MeOH, r.t.): λ_{max} (ε, M^{-1} cm^{-1}) = 681 (129) nm.

[CuL^{4}Cl(H$_2$O)]ClO$_4$·H$_2$O (4-Cl): **L^4**·xHCl (0.26 g, 0.50 mmol), $Cu(ClO_4)_2 \cdot 6H_2O$ (0.20 g, 0.54 mmol), methanol (15 mL), green solid (0.38 g, 0.47 mmol, 94.00%). M.p. 138–150 °C (dec.). The compound was not isolated in pure form and probably consists of a mixture of **4** and **4**-Cl. UV/Vis (d–d transition in MeOH, r.t.): λ_{max} (ε, M^{-1} cm^{-1}) = 696 (90) nm. A few green X-ray quality crystals were obtained from crystallization from ethyl acetate/acetonitrile at –20 °C.

Biological Assays: The murine (P388, Raw 264.7, WEHI-3) and human (K562) leukemia cell lines, as well as the murine lung fibrosarcoma L929, were acquired from ATCC. Cells were cultivated in IMDM (Gibco, BRL, USA) supplemented with 10% FBS (Gibco, BRL, USA) and penicillin at 37 °C, 5% CO_2, and humidity at dew-point level. Biological assays were carried out with cells in 96 well plates, with initial densities of 5×10^4, 3×10^5, 1.2×10^5, 2.5×10^5, and 2×10^5 cells/mL of WEHI-3, P388, Raw 264.7, K562, and L929, respectively; we also employed 1×10^5 cells/mL with rmIL-3 (5 ng/mL) of normal mononuclear cell from Balb/c mouse bone marrow as control. Complexes **1**–**4** were evaluated at 1.5, 3, 7.5, 15, 30, 60, and 120 μM, and cisplatin was used as reference. The inhibitory effect on proliferation was evaluated after 72 h for malignant cell lines and 120 h for healthy bone marrow cells by the sulforhodamine B method,[29] as a measure of the cytotoxicity. Data are presented as the mean value ± the standard deviation of the proliferation percent of at least three independent assays, each repeated four times.

Supporting Information (see footnote on the first page of this article): Proliferation inhibition studies, cyclic voltammograms, and EPR spectra.

Acknowledgments

The authors thank Carmen Márquez and Luis Velasco for mass spectrometry measurements, Eréndira García Ríos for combustion analysis, Elizabeth Huerta and Rocío Patiño for IR and UV/Vis determinations, Virginia Gómez-Vidales for EPR spectroscopy, and Dirección General de Asuntos del Personal Académico, Universidad Nacional Autónoma de México (DGAPA-UNAM) for financial support (IN211509).

[1] a) C. Orvig, M. J. Abrams, *Chem. Rev.* **1999**, *99*, 2201–2203; b) Z. Guo, P. J. Sadler, *Angew. Chem. Int. Ed.* **1999**, *38*, 1512–1531.
[2] a) B. Rosenberg, *Platinum Met. Rev.* **1971**, *15*, 42–51; b) R. A. Alderden, M. D. Hall, T. W. Hambley, *J. Chem. Educ.* **2006**, *83*, 728–734.
[3] a) C. X. Zhang, S. J. Lippard, *Curr. Opin. Chem. Biol.* **2003**, *7*, 481–489; b) L. R. Kelland, *Drugs* **2000**, *59*, 1–8.
[4] M. Frezza, S. Hindo, D. Chen, A. Davenport, S. Schmitt, D. Tomco, Q. P. Dou, *Curr. Pharm. Des.* **2010**, *16*, 1813–1825.
[5] a) T. Wang, Z. Guo, *Curr. Med. Chem.* **2006**, *13*, 525–537; b) M. C. Linder, *Biochemistry of Copper*, Plenum Press, New York, **1991**.
[6] S. S. Hindo, M. Frezza, D. Tomco, M. J. Heeg, L. Hryhorczuk, B. R. McGarvey, Q. P. Dou, C. N. Verani, *Eur. J. Med. Chem.* **2009**, *44*, 4353–4361.
[7] a) C. Marzano, M. Pellei, F. Tisato, C. Santini, *Anti-Cancer Agents Med. Chem.* **2009**, *9*, 185–211; b) S. Tardito, L. Marchiò, *Curr. Med. Chem.* **2009**, *16*, 1325–1348.
[8] S. Tardito, I. Bassanetti, C. Bignardi, L. Elviri, M. Tegoni, C. Mucchino, O. Bussolati, R. Franchi-Gazzola, L. Marchiò, *J. Am. Chem. Soc.* **2011**, *133*, 6235–6242.
[9] B. J. Hathaway in *Comprehensive Coordination Chemistry* (Eds.: G. Wilkinson, R. D. Gillard, J. A. McCleverty), Pergamon Press, Oxford, **1987**, vol. 5, pp. 533–594.
[10] W. E. Antholine, J. M. Knight, D. H. Petering, *J. Med. Chem.* **1976**, *19*, 339–341.
[11] J. Easmon, G. Puerstinger, G. Heinisch, T. Roth, H. H. Fiebig, W. Holzer, W. Jaeger, M. Jenny, J. Hofmann, *J. Med. Chem.* **2001**, *44*, 2164–2171.
[12] a) A. Marzotto, A. Ciccarese, D. A. Clemente, G. Valle, *J. Chem. Soc., Dalton Trans.* **1995**, 1461–1468; b) M. B. Ferrari, S. Capacchi, G. Pelosi, G. Reffo, P. Tarasconi, R. Albertini, S. Pinelli, P. Lunghi, *Inorg. Chim. Acta* **1999**, *286*, 134–141; c) P. de Hoog, M. J. Louwerse, P. Gamez, M. Pitié, E. J. Baerends, B. Meunier, J. Reedijk, *Eur. J. Inorg. Chem.* **2008**, 612–619.
[13] D. S. Sigman, R. Landgraf, D. M. Perrin, L. Pearson, *Met. Ions Biol. Syst.* **1996**, *33*, 485–513.
[14] a) P. J. Jansson, P. C. Sharpe, P. V. Bernhardt, D. R. Richardson, *J. Med. Chem.* **2010**, *53*, 5759–5769; b) S. Zhang, Y. Zhu, C. Tu, H. Wei, Z. Yang, L. Lin, J. Ding, J. Zhang, Z. Guo, *J. Inorg. Biochem.* **2004**, *98*, 2099–2106.
[15] a) M. Andrzejewska, L. Yepez-Mulia, R. Cedillo-Rivera, A. Tapia, L. Vilpo, J. Vilpo, Z. Kazimierczuk, *Eur. J. Med. Chem.* **2002**, *37*, 973–978; b) S.-T. Huang, L.-J. Hsei, C. Chen, *Bioorg. Med. Chem.* **2006**, *14*, 6106–6119.
[16] a) M. Devereaux, M. McCann, D. O. Shea, R. Kelly, D. Egan, C. Deegan, K. Kavanagh, V. McKee, G. Finn, *J. Inorg. Biochem.* **2004**, *98*, 1023–1031; b) M. Devereaux, D. O. Shea, A. Kellett, M. McCann, M. Walsh, D. Egan, C. Deegan, K. Kedziora, G. Rosair, H. Müller-Bunz, *J. Inorg. Biochem.* **2007**, *101*, 881–892.
[17] P. R. Martínez-Alanis, M. López Ortiz, I. Regla, I. Castillo, *Synlett* **2010**, 423–426.
[18] V. O. Rodionov, S. I. Presolski, S. Gardinier, Y.-H. Lim, M. G. Finn, *J. Am. Chem. Soc.* **2007**, *129*, 12696–12704.
[19] R. Mukherjee in *Comprehensive Coordination Chemistry II* (Eds.: J. A. McCleverty, T. J. Meyer), Elsevier, Amsterdam, **2004**, vol. 6, pp. 747–910.
[20] M. Kodera, T. Kita, I. Miura, N. Nakayama, T. Kawata, K. Kano, S. Hirota, *J. Am. Chem. Soc.* **2001**, *123*, 7715–7716.
[21] D. Wahnon, R. C. Hynes, J. Chin, *J. Chem. Soc., Chem. Commun.* **1994**, 1441–1442.
[22] a) P. E. Pjura, K. Grzeskoviak, *J. Mol. Biol.* **1987**, *197*, 257–271; b) F. G. Lootiens, P. Regenfuss, A. Zechel, L. Dumortier, R. M. Clegg, *Biochemistry* **1990**, *29*, 9029–9039.
[23] M. Chikira, Y. Tomizawa, D. Fukita, T. Sugizaki, N. Sugawara, T. Yamazaki, A. Sasano, H. Shindo, M. Palaniandavar, W. E. Antholine, *J. Inorg. Biochem.* **2002**, *89*, 163–173.
[24] F. Arnesano, G. Natile, *Coord. Chem. Rev.* **2009**, *253*, 2070–2081.
[25] a) T. B. Thederahn, M. D. Kuwabara, T. A. Larsen, D. S. Sigman, *J. Am. Chem. Soc.* **1989**, *111*, 4941–4946; b) M. Pitie, C. Boldron, G. Pratviel, *Adv. Inorg. Chem.* **2006**, *58*, 77–130; c) N. Aliaga-Alcalde, P. Marqués-Galleo, M. Kraaijkamp, C. Herranz-Lancho, H. den Dulk, H. Gorner, O. Roubeau, S. J. Teat, T. Weyhermuller, J. Reedijk, *Inorg. Chem.* **2010**, *49*, 9655–9663; d) S. S. Bhat, A. A. Kumbhar, H. Heptullah, A. A. Khan, V. V. Gobre, S. P. Gejji, V. G. Puranik, *Inorg. Chem.* **2011**, *50*, 545–558.
[26] Bruker AXS, *SAINT* Software Reference Manual v. 6.23C, Madison, **2002**.
[27] G. M. Sheldrick, *SHELXS-97: Crystal Structure Solution*, University of Göttingen, Germany, **1990**.
[28] G. M. Sheldrick, *SHELXL-97: Crystal Structure Refinement*, University of Göttingen, Germany, **1997**.
[29] V. Vichai, K. Kirtikara, *Nat. Protoc.* **2006**, *1*, 1112–1116.

Received: March 24, 2011
Published Online: July 12, 2011

